Article:
Garcia, RR, López-Puertas, M, Funke, B et al. (2016) On the secular trend of CO_x and CO_2 in the lower thermosphere. Journal of Geophysical Research: Atmospheres, 121 (7). pp. 3634-3644. ISSN: 2169-897X

https://doi.org/10.1002/2015JD024553

On the secular trend of CO_x and CO_2 in the lower thermosphere

Rolando R. Garcia[1], Manuel López-Puertas[2], Bernd Funke[2], Douglas E. Kinnison[1], Daniel R. Marsh[1], and Liying Qian[1]

[1]National Center for Atmospheric Research, Boulder, CO, USA

[2]Instituto de Astrofísica de Andalucía, CSIC, Granada, Spain

Corresponding author: R. R. Garcia, National Center for Atmospheric Research, Boulder, CO, 80307-3000, USA (rgarcia@ucar.edu)

Key points:

- Observations suggest that CO_2 in the lower thermosphere has increased rapidly since the early 2000s.
- The observed behavior cannot be simulated by a comprehensive climate-chemistry model.
- Model and observations could be reconciled if vertical eddy mixing has increased by about 30% per decade.

Abstract

An analysis of recent observations (2004-2013) made by the ACE-FTS instrument indicate that total carbon ($CO_x = CO + CO_2$) has been increasing rapidly in the lower thermosphere, above 10^{-3} hPa (90 km). The estimated trend (~9% per decade) is about a factor of two larger than the rate of increase that can be ascribed to anthropogenic emissions of CO_2 (~5% per decade). Here we investigate whether the observed trends of CO_2 and CO_x can be reproduced using the Whole Atmosphere Community Climate Model (WACCM), a comprehensive global model with interactive chemistry, wherein vertical eddy diffusion is estimated from a parameterization of gravity wave breaking that can respond to changes in the model climate. We find that the modeled trends of CO_2 and CO_x do not differ significantly at any altitude from the value expected from anthropogenic increases of CO_2, and that WACCM does not produce significant changes in eddy diffusivity. We show that the discrepancy between model and observations cannot be attributed to uncertainties associated with geophysical noise and instrumental effects, to difficulties separating a linear trend from the 11-year solar signal, or to sparse sampling by ACE-FTS. Estimates of the impact of vertical diffusion on CO_2 in the model indicate that a large increase in K_{zz} (~30% per decade) would be necessary to reconcile WACCM results with observations. It might be possible to ascertain whether such a large change in vertical mixing has in fact taken place by examining the trend of water vapor in the upper mesosphere.

1. Introduction.

Emmert et al. (2012) calculated the global linear trend of CO_x (the sum of CO and CO_2) from observations made by the Atmospheric Chemistry Experiment Fourier Transform Spectrometer (ACE-FTS) between April 2004 and September 2011, and documented a very fast rate of increase at altitudes above about 10^{-3} hPa (~90 km). Near 100 km, the linear trend of CO_x was approximately 9% per decade, which is much faster than the anthropogenic rate of increase of CO_2 in the lower atmosphere for the period in question (~5% per decade). *Emmert et al.* analyzed the trend in CO_x in order to minimize the effects of the solar cycle on CO_2, since the photolysis of this gas by UV radiation (which produces CO) becomes important above 90 km and varies strongly with solar activity. Insofar as CO_2 represents the bulk of CO_x below about 100 km, *Emmert et al.* ascribed the trend in CO_x to increases in CO_2. They also showed, using a one-dimensional model with interactive chemistry [*Roble*, 1995], that the observed trend in CO_x could be due to a corresponding trend in vertical eddy diffusion of 15% per decade, since such a trend would increase the rate of transport of CO_2 into the lower thermosphere. Indeed, *Garcia et al.* [2014] have shown that, in the range of altitude 90-105 km (about 10^{-3} to 10^{-4} hPa), the mixing ratio of CO_2 is controlled principally by the competition between eddy diffusion and molecular diffusive separation.

Emmert et al.'s conclusions regarding a fast rate of increase of CO_2 in the lower thermosphere are supported by the recent study of *Yue et al.* [2015], who used SABER (Sounding of the Atmosphere by Broadband Emission Radiometry) observations from 2002 through 2014, and estimated a rate of increase of CO_2 exceeding 10% per decade above 100 km. While SABER observations do not include CO, *Yue et al*. performed a multiple

linear regression that included the solar 10.7 cm radio flux as a predictor to account for the influence of solar activity on CO_2.

Here we investigate whether the large trends of CO_2 and CO_x in the upper atmosphere derived from observations can be reproduced in simulations made with the Whole Atmosphere Community Climate Model (WACCM), a three-dimensional, global climate model with interactive chemistry. The model is discussed briefly in Section 2, with emphasis on the question of transport in the mesosphere and lower thermosphere (MLT), which is dominated by the divergence of vertical eddy fluxes due to breaking gravity waves. While these small-scale waves cannot be simulated explicitly at the relatively coarse spatial and temporal resolutions used in a climate model, they are parameterized in such a way that they can respond to changes in the model's climate.

In Section 3, we compare updated ACE-FTS observations that span the period 2004 through 2013 with WACCM simulations of the same period to show that the simulated CO and CO_2 agree well with the observations in the lower thermosphere. In Section 4, we derive trends in CO_x and CO_2 from the ACE-FTS data and compare them with trends derived from WACCM output, and with the earlier estimates of *Emmert et al.* [2012]. The trends derived from the data are consistent with the findings of *Emmert et al.*, and are much larger than the model trends above 90 km. In fact, WACCM-derived trends in the lower thermosphere are not significantly different from the trends below the mesopause, which are ascribable to anthropogenic emissions of CO_2. We go on to examine several possible sources of uncertainty that might account for the discrepancy between observed and modeled trends, and conclude that none can explain the differences between the model and the observations. Finally, we estimate the impact of increases in vertical eddy diffusion on

93 the trends computed with WACCM, and find that a rather large K_{zz} trend, of over 30% per
94 decade, would be needed to reconcile the model with the observations. In Section 5, we
95 summarize our findings and suggest additional observations that might be useful for
96 ascertaining whether such increases in vertical eddy diffusion might have taken place in the
97 Earth's upper atmosphere.

98 **2. Numerical model**

99 The Whole Atmosphere Community Climate Model (WACCM) is a global climate
100 model with interactive chemistry that spans the range of altitude 0-140 km. In this study,
101 we use the "specified dynamics" version (SD-WACCM), described by *Garcia et al.* [2014].
102 In SD-WACCM, winds and temperature are constrained by NASA's Modern-Era
103 Retrospective Analysis (MERRA) data [*Rienecker et al.,* 2011] everywhere below
104 approximately 1 hPa, using the procedure discussed by *Kunz et al.* [2011]. The use of SD-
105 WACCM for the present investigation is motivated by the desire to study the particular
106 period, 2004 through 2013, covered by the ACE-FTS observations described in the next
107 section. While SD-WACCM is free running above 1 hPa, *Liu et al.* [2009] have shown that
108 the dynamics of the mesosphere and lower thermosphere are strongly influenced by the
109 behavior of the lower atmosphere. In the remainder of this paper, we refer to the model
110 simply as WACCM, with the understanding that all simulations have been carried out with
111 the specified dynamics version.

112 The reader is referred to the study of *Garcia et al.* [2014] for additional details of the
113 specified dynamics configuration. Here, we emphasize only the parameterization of small-
114 scale gravity waves, since vertical mixing due to gravity wave breaking is the principal

upward transport mechanism in the lower thermosphere, below 10^{-4} hPa, particularly in the global-mean sense. The gravity wave parameterization attempts to take into account the excitation of mesoscale waves by various physical mechanisms, such as flow over orography, deep convection, and frontal zones. Non-orographic gravity wave source spectra are dependent on convective heat release in the Tropics and frontal zones diagnosed in extra-tropical latitudes, as described in detail by *Richter et al*. [2010]. Because parameterized gravity wave sources are related to physical processes simulated in the underlying global model, their behavior can potentially change as the model climate changes. For example, the source spectra will change if the characteristics of convection or the frequency or intensity of fronts diagnosed in the model changes; and the propagation of the waves to the MLT will be influenced by the behavior of the zonal-mean zonal wind systems in the stratosphere.

We note that the effective value of K_{zz} calculated with WACCM depends also on the value assumed for the Prandtl number, *Pr*, which describes the ratio of the eddy momentum flux to the eddy flux of potential temperature or chemical species [see *Garcia et al.*, 2007]. The value used in the study of *Garcia et al.* [2014] was $Pr = 4$. As discussed in that study, comparison of simulated and observed CO and CO_2 suggests that a smaller value, $Pr = 2$, might be more appropriate; therefore, we use simulations made with $Pr = 2$ to compute model trends in this study. Nevertheless, in Section 4 we use results from our earlier simulation with $Pr = 4$ to estimate the potential impact of changes in K_{zz} on the trends of CO_x and CO_2. (It should be ~~noted~~emphasized, however, that the trends of CO_2 and CO_x in WACCM are insensitive to *Pr* as long as the value of *Pr* is constant throughout the simulation).

3. Comparison of observed and modeled CO and CO_2

The Atmospheric Chemistry Experiment Fourier Transform Spectrometer (ACE-FTS) on SCISAT-1 has been making solar occultation measurements of CO and CO_2 since 2004 [*Boone et al*., 2005; *Clerbaux et al.,* 2008; *Beagley et al.,* 2010]. CO_2 volume mixing ratio (vmr) is retrieved from 50 to 120 km; the vertical resolution averages 3-4 km, varying from 2 to 6 km depending on the time of the year. Random errors are 2.5-5%, depending on latitude, and systematic errors range from 2% at the low altitudes (50-70 km) to about 5% at 90 km, 9% at 100 km, and 16% at 118.5 km [*Beagley et al.,* 2010]. CO vmr is retrieved in the range from 8 km to about 100 km [*Clerbaux et al.*, 2008]. The vertical resolution above about 1 hPa is about 4 km, degrading to 6 km in the upper mesosphere. The random errors of the CO measurements are < 10% in the mesosphere and lower thermosphere; systematic errors are < 25% from 30 to 100 km. The ACE-FTS observations, as well as the data screening procedures employed, are discussed in more detailed by *Garcia et al*. [2014]. The data used here is version 3.5 [*Boone et al.,* 2013] and was obtained from the ACE Science Team at the University of Waterloo, Canada. We note that ACE observations are processed in geometric coordinates. However, the final data products are provided in both geometric and pressure coordinates, and we use data in pressure coordinates in all comparisons with WACCM.

CO has also been observed by the Michelson Interferometer for Passive Atmospheric Sounding (MIPAS) using the "middle atmosphere" and "upper atmosphere" modes [*Oelhaf*, 2008], which cover the altitude ranges 20-102 km and 40-170 km, respectively. The vertical resolution of the MIPAS CO profiles is 4–7 km below 60 km at night and below 95 km during daytime, and 7-14 km above those altitudes. The single-measurement

precision (noise error) is 40-80% below 60 km, and 30-60% above, while the systematic error is estimated to range between 8 and 15 % [*Funke et al.,* 2009]. The MIPAS data are also discussed in detail by *Garcia et al.* [2014].

Figure 1 shows time series of WACCM CO and CO_2 together with observations at several levels in the lower thermosphere: 6×10^{-5} hPa (~108 km), 2×10^{-4} hPa (~100 km) and 10^{-3} hPa (~90 km). For CO_2, WACCM is within 10% of the ACE-FTS observations at all levels except 6×10^{-5} hPa, where the differences reach 15-20%. While the discrepancies are not large compared to the measurement errors for ACE-FTS, WACCM results for CO_2 are uniformly low in all cases. For CO, the WACCM simulation is generally closer to observations, especially given the large measurement errors. However, at 10^{-3} hPa, WACCM CO is systematically higher than both ACE-FTS and MIPAS. In spite of these discrepancies, WACCM reproduces well the long-term variability of the data, which is dominated by the solar cycle, in particular at the higher altitudes.

The effect of the solar cycle can be largely removed by considering total carbon, CO_x, which in the lower thermosphere is essentially the sum of CO and CO_2. Figure 2 shows a comparison of modeled and observed CO_x at 10^{-3} and 2×10^{-4} hPa, two levels where both CO and CO_2 are measured by ACE-FTS. Since CO_x at these levels is dominated by CO_2, the agreement is within 10%, as was the case for CO_2 in Figure 1, with WACCM being systematically low compared to ACE-FTS. In both model and observations, the evolution of CO_x shows mainly an increasing trend, with no indication of any solar cycle influence. The rate of increase of CO_x is clearly faster in ACE-FTS than in WACCM, and this difference will be quantified in the next section, where we calculate linear trends. An additional difference between model and observations, both for CO_x and for CO and CO_2

individually, is that the observations exhibit considerably larger short-term variability than the model. The potential effect of this difference on the calculation of trends from WACCM output will be addressed below.

4. Calculation and comparison of linear trends

Time series of CO_x in WACCM are constructed from monthly-mean, globally averaged output for CO and CO_2. The model output was de-seasonalized by subtracting the composite monthly seasonal cycle for the period 2004-2013 at each model level. ACE-FTS data were treated here in the same way as the WACCM output; that is, de-seasonalized, global monthly averages were calculated from the data on each pressure level. This differs from the procedure employed by *Emmert et al.* [2012] but yields very similar trends, as shown below.

We characterize the long-term behavior of CO_x in the 10-year period 2004 to 2013 in terms of the linear trend obtained from a multiple linear regression (MLR). The regression model used is:

$$\psi = a + b \cdot t + c \cdot s(t) + d \cdot qbo_1(t) + e \cdot qbo\_2(t) \qquad (1)$$

where t is time; s is a solar cycle predictor, here taken to be the 10.7 cm radio flux; and qbo_1, and qbo_2 are two linearly independent indices of the quasi-biennial oscillation (QBO), represented by the zonal-mean zonal wind at 10 and 30 hPa, respectively. The autocorrelation of the residuals of the fit was taken into account when estimating the uncertainty of the trend [*Tiao et al.,* 1990]. No attempt was made to include in the MLR predictors for ENSO (El Niño-Southern Oscillation) or for volcanic eruptions. In practice, it turns out that even the QBO predictors explain a negligible fraction of the variance of CO_x

206 in the lower thermosphere. Likewise, the solar predictor turns out to be relatively
207 unimportant at the altitudes (below about 105 km) where CO_x data are available from ACE-
208 FTS. Note that this is not true of CO_2 alone, which is photolyzed by UV radiation to
209 produce CO. However, the combination of CO and CO_2 into a total carbon variable, CO_x,
210 has the desirable effect of minimizing the impact of the solar cycle on the MLR.

211 Figure 3 compares the vertical profile of the linear trend coefficient, *b,* obtained when
212 the MLR defined by Eq. (1) is applied to ACE-FTS observations and to WACCM output.
213 Three things are immediately obvious from the figure: The trend calculated from ACE-FTS
214 measurements reaches a maximum of 8.5% at 95-100 km, consistent with the results of
215 *Emmert et al.* [2002], who analyzed a shorter period (2004-2011); the trend calculated from
216 WACCM output in the lower thermosphere is statistically indistinguishable from the trend
217 at lower altitudes; and the WACCM trend is significantly different from that derived from
218 ACE-FTS observations in the lower thermosphere, between 2 x 10^{-3} hPa (~85 km) and 2 x
219 10^{-4} hPa (~100 km). As in *Emmert et al.*, our estimate of the ACE-FTS trend below 80 km
220 (~10^{-2} hPa) is influenced by *a priori* assumptions about CO_2 inherent in the ACE-FTS
221 retrieval, which yield too low a trend for the period under examination. However, as noted
222 by *Emmert et al.*, this does not affect the estimate of the trend above 90 km (~10^{-3} hPa).

223 We consider next whether the statistical significance of the WACCM-ACE differences
224 might be exaggerated because WACCM CO_x has substantially less short-term variability
225 than ACE-FTS data. Specifically, the WACCM time series shown in Figures 1 and 2 are
226 constructed from true zonal means averaged globally over latitude, whereas ACE-FTS solar
227 occultation observations are much more sparse, both in longitude and latitude, and in time,
228 and they are subject to measurement errors not present in WACCM. A cursory

examination of Figures 1 and 2 reveals that the high-frequency variability is about a factor of 2 larger in the ACE-FTS time series than in the WACCM time series. We therefore test the sensitivity of the WACCM trends to the addition of "random noise", which we simulate simply by adding to the time series of WACCM CO and CO_2 a series of normally distributed pseudo-random numbers, multiplied times the standard deviation of the original time series at each altitude; this has the effect of increasing the standard deviation of the resulting "noisy" time series by about a factor of $\sqrt{2}$ compared to the original. As a result, the high-frequency variability of the treated WACCM output is similar to that seen in ACE-FTS data (not shown). The linear CO_x trend profile extracted from the WACCM output with added noise is shown in Figure 4. While the uncertainty of the trend is much larger than for the original WACCM output (Figure 3) the trend in the thermosphere remains statistically undistinguishable from the trend at lower altitudes, and statistically different from the ACE-FTS trend between about 85 and 100 km.

We have also tested whether uncertainties in our knowledge of 11-year solar variability at UV wavelengths might influence the CO_x trend derived from WACCM. As discussed by *Ermolli et al.* [2013], recent measurements of spectral solar irradiance (SSI) variability differ substantially from estimates based on empirical models. In particular, *Ball et al*. [2014] show that the 11-year variability observed by the SOLSTICE instrument onboard NASA's SORCE satellite is much larger at wavelengths < 300 nm than predicted by models such as NRLSSI [*Lean et al.,* 1997] and SATIRE [*Krivova et al.,* 2011]. For CO_x, we are interested in the range of wavelength 121-200 nm, which dominates CO_2 photolysis below ~105 km [cf. *Garcia et al.*, 2014; their Figure 1]. At these wavelengths, SSI changes over the 11-year solar cycle are about a factor of two larger in SOLSTICE observations

252 than in either of the aforementioned models. SSI in WACCM is prescribed using the
253 NRLSSI model, so we adjusted SSI variability in the range 120-200 nm to be twice as
254 predicted by this model, with no changes elsewhere in the spectrum, and carried out a new
255 simulation of the period 2004-2013. The resulting CO_x trend profile is compared with the
256 original trend profile in Figure 5. It is evident that the larger SSI variability at 120-200 nm
257 introduces little additional uncertainty in the WACCM CO_x trend, even at 100 km. This is
258 not wholly surprising because the use of CO_x is intended to minimize the effect of solar
259 variability on the estimate of the long-term trend. In addition, as shown by *Garcia et al.*
260 [2014] (cf. their Figure 9), the mixing ratio of CO_2 below 10^{-4} hPa (~105 km) is determined
261 mainly by the competition between vertical eddy diffusion due to gravity wave breaking
262 and molecular diffusive separation, with a smaller influence from UV photolysis.

263 Finally, we have considered whether the sparse sampling inherent in solar occultation
264 observations might contribute to the differences in the trend profiles derived from ACE-
265 FTS and WACCM. To investigate this possibility, we extracted WACCM vertical profiles
266 of CO and CO_2 at the geo-locations (longitude, latitude, and time) nearest to ACE-FTS
267 observations for the period 2004-2013. We then performed a trend analysis after processing
268 the data as described by *Emmert et al.* [2012], with one exception: we regressed the
269 WACCM output on both time (the linear trend) and on the solar f10.7 cm radio flux. As
270 noted previously, regression on a solar predictor does not affect the results below 10^{-4} hPa
271 (~105 km), although it becomes increasingly important at higher altitudes, where CO_x is no
272 longer conserved due to differences in molecular diffusion between CO and CO_2. The
273 resulting trend profile is shown in Figure 6. It is clear that, even when the model is sampled

using the ACE geo-locations, the WACCM trend is significantly smaller than the ACE-FTS trend at altitudes between about 85 and 100 km.

5. Summary and Discussion

The results presented above show that the global trend of CO_x in the lower thermosphere calculated with WACCM is not significantly different from the trend ascribable to anthropogenic increases in CO_2, and that this trend (nowhere larger than 5.5%) is much smaller than the trend calculated from ACE-FTS observations (8-9% per decade in the lower thermosphere). We have also shown that, even when we consider several plausible sources of uncertainty that might affect the WACCM CO_x trend, that trend remains smaller and statistically different from the ACE-FTS trend in the lower thermosphere.

Emmert et al. [2012] suggested that the CO_x trend derived from ACE-FTS observations could be explained if the rate of eddy diffusive transport of CO_2 into the lower thermosphere was itself increasing. We have examined the evolution of the vertical diffusion coefficient, K_{zz}, estimated from the gravity wave parameterization in WACCM and find no statistical significant trend anywhere in the model domain during the period under consideration, 2004-2013; this is consistent with the lack of any trend in CO_2 or CO_x in the model beyond that due to anthropogenic emissions.

The value of K_{zz} in WACCM is predicted by the gravity wave parameterization interactively with the underlying, resolved dynamics, and cannot easily be adjusted *ad hoc*. However, we can estimate the impact of K_{zz} on chemical species by comparing otherwise identical simulations made with a different value of the Prandtl number, *Pr,* which

296 describes the ratio of the eddy momentum flux to the eddy flux of chemical species [see
297 *Garcia et al*., 2007]. In particular, halving *Pr* has the effect of increasing the effective
298 magnitude of K_{zz} by approximately a factor of two. As noted in Section 2, the simulations
299 examined thus far were made using $Pr = 2$, but we also have at hand earlier simulations,
300 discussed by *Garcia et al.* [2014], that used $Pr = 4$. By comparing CO and CO_2 across the
301 simulations, we can ascertain the impact of doubling K_{zz} on these species. Then, if we
302 assume that changes in CO and CO_2 are linear in K_{zz}, we can estimate the impact of smaller
303 changes in K_{zz} acting over one decade, and thus estimate the decadal trend in eddy diffusion
304 that is necessary to bring WACCM CO_x trends into agreement with ACE-FTS trends.

305 Figure 7 shows the estimated effect on the WACCM CO_x trend of increasing K_{zz} at
306 various rates. The figure reproduces the trend results shown earlier in Figure 3,
307 superimposing upon those our estimates of the trends that would result if K_{zz} in WACCM
308 increased at 25%, 33% and 50% per decade. Above about 10^{-2} hPa, where CO_2 is no longer
309 well mixed, changes in K_{zz} begin to impact the CO_x trend, and a trend of 33% per decade in
310 K_{zz} gives the best match to the observed trend in CO_x below about 2×10^{-4} hPa (95 km).
311 Above that altitude there are substantial differences between the estimated WACCM trend
312 and the ACE-FTS trend; better agreement might have been achieved by limiting the altitude
313 range over which K_{zz} changes, but we have avoided any such arbitrary modifications, if for
314 no other reason that they would have required additional calculations that are not easily
315 implemented in the model. A similar mismatch between the modeled and observed trend
316 profiles occurred when *Emmert et al.* used a one-dimensional model to support their
317 argument for an increase in the rate of vertical diffusion (cf. their Figure 2). Thus, neither
318 the results presented in Figure 7 nor those of *Emmert et al.* produce a completely

satisfactory agreement between modeled and observed trends of CO_x, although they are able to match the observed trends over much of the lower thermosphere.

Similar results are obtained when trends in CO_2 alone are considered, as shown in Figure 8. Again, a decadal increase in K_{zz} of about a third would bring the WACCM trend of CO_2 into line with the trend obtained from ACE-FTS data. Incidentally, the ACE-FTS trend of CO is statistically indistinguishable from zero everywhere above 90 km (not shown). Thus, the discrepancy in modeled versus observed trends in CO_x is dominated by the behavior of CO_2, at least below 100-105 km, where most of the total carbon resides in CO_2. The very large trend in CO_2 obtained from ACE-FTS data (which exceeds 12% near 105 km) is consistent with the recent study of *Yue et al.* [2015], who estimated the trend in CO_2 from observations made by the SABER instrument onboard NASA's TIMED satellite from 2002 through 2014. *Yue et al.* reported a trend of ~10% per decade above 105 km; as shown in their Figure 2, the trend profile derived from SABER differs from the ACE-FTS trend profile in that the trend peaks at a higher altitude, but is consistent with ACE-FTS insofar as the trend in the lower thermosphere is much larger than the trend below 80 km.

Taken together, the SABER and ACE-FTS results make a strong case for a fast increase in CO_2 in the lower thermosphere in recent years. WACCM simulations, on the other hand, produce trends that are everywhere indistinguishable from the trend at lower altitudes, which can be ascribed to anthropogenic emissions of CO_2. Estimates of the impact of K_{zz} on modeled trends suggest that an increase in eddy vertical mixing can bring the model results into agreement with observations. This is consistent with the conclusions of *Emmert et al.* [2012], who obtained a similar result using the one-dimensional, diffusive model of *Roble* [1995]. The required change in K_{zz} ranges from 15% per decade in the

calculations of *Emmert et al.* to over 30% per decade in the estimates presented here. The parameterization of gravity wave breaking included in WACCM is designed to interact with the resolved dynamics of the underlying model, as discussed in Section 2, but fails to produce a significant change in K_{zz} in the MLT over the period considered here (or indeed, over any period in the late 20th and early 21st centuries; not shown). Furthermore, there is essentially no direct evidence for a recent global increase in turbulent mixing, although the work of *Hoffman et al.* [2011] suggests a local increase in gravity wave activity over Juliusruh, Germany (55°N).

In view of the foregoing results, one might wonder whether it is possible to find additional, independent evidence for a rapid increase in eddy vertical mixing in the MLT since the early 2000s. Insofar as there are no global, long-term observations of gravity wave breaking in the MLT, evidence for a global increase in K_{zz} would have to come from global observations of minor species that are expected to respond sensitively to vertical mixing. We have examined the impact of K_{zz} in WACCM on several species, including atomic oxygen (which can be estimated from ozone and OH airglow observed by SABER, and is measured by the SC~~H~~IAMACHY instrument on the Envisat satellite [*Zhu et al.*, 2015]), and water vapor (which has been measured by SABER but not yet released as a validated data product). As regards atomic oxygen, Smith et al. (2009) have shown that its vertical profile is affected by vertical diffusion. However, w~~W~~e find that, even though O exhibits a very steep vertical gradient above 80 km, it is not very sensitive to changes in K_{zz} in WACCM. This happens because the vertical gradient of O is shallow at the altitudes where its photochemical lifetime is long, and steep mainly where it photochemical lifetime is short, which reduces the impact of transport on the local mixing ratio. Even a 50%

365 change in K_{zz} produces changes in WACCM O whose magnitude is less than 10% (not
366 shown).

367 Water vapor, on the other hand, may be a potentially useful indicator of changes in K_{zz}.
368 Water vapor is photolyzed by Lyman-alpha radiation above about 80 km, but the rate of
369 photolysis is slow enough (days to weeks) that the vertical gradient is strongly influenced
370 by eddy mixing. Figure 9 shows the estimated impact of trends in K_{zz} on the trend of water
371 vapor. Between about 85 and 95 km (3×10^{-3} to 5×10^{-4} hPa), where the H_2O mixing ratio
372 in WACCM varies from about 1 ppmv to 0.5 ppmv (not shown), a 33% per decade trend in
373 K_{zz} would produce a trend in H_2O varying from 15% per decade at 85 km to 30% per
374 decade at 95 km. This is substantially larger than the trend below the mesopause (~7% per
375 decade), which in WACCM arises mainly from specified anthropogenic emissions of
376 methane and a slight warming of the cold point tropopause during the period of interest.
377 Above 95 km, the trend in H_2O produced by increasing K_{zz} is even larger than at lower
378 altitudes, but the local mixing ratio is much less than 1 ppmv, likely making it impossible to
379 retrieve its abundance accurately.

380 *Nedoluha et al.* [2009] studied the evolution of water vapor in the mesosphere, up to
381 about 80 km, during solar cycle 23. They compared observations made by the Water Vapor
382 Millimeter-wave Spectrometer (WVMS) with data from HALOE (Halogen Occultation
383 Experiment) and other instruments that together covered the period 1992-2008. After
384 accounting for the impact of changes in Lyman-alpha radiation over the solar cycle,
385 *Nedoluha et al.* found that HALOE water vapor increased by about 8-9% between 60 and
386 80 km from 1992 through 1996; on the other hand, from 1996 through 2005 (the last year
387 of HALOE observations), water vapor decreased slightly in both HALOE and WVMS. To

put these findings in perspective, the WACCM water vapor trend over the decade 1992-2001 (which encompasses the period of increase documented by *Nedoluha et al.*), is ~8 ± 7% at 80 km and ~13 ± 12% at 90 km (not shown); this may be compared to the nearly altitude independent 7 ± 10% per decade obtained for 2004-2013 (Figure 9). The trend in K_{zz} calculated by WACCM over the period 1992-2001 is also statistically indistinguishable from zero (not shown). Evidently, WACCM water vapor can exhibit substantial inter-decadal variability, comparable to that seen in the observations analyzed by *Nedoluha et al*., that is unrelated to eddy transport and could complicate the attribution of decadal trends. Nevertheless, the estimated impact of changes in K_{zz} illustrated in Figure 9 is large enough (15-30% per decade at 85-95 km) that it ought to be discernible even in the presence of variability arising from other sources.

In summary, the evidence from the observations considered in this study points to a fast rate of increase in CO_2 in the lower thermosphere that cannot be simulated with our state of the art climate-chemistry model. In order for WACCM to produce trends of CO_x and CO_2 in the lower thermosphere consistent with ACE-FTS and SABER observations, vertical eddy diffusion would have to increase substantially (at an estimated rate of over 30% per decade). Examination of suitable datasets for other minor species (e.g., water vapor) in the lower thermosphere would be desirable to provide independent confirmation of such a rapid rate of increase in turbulent mixing.

Acknowledgments. The Atmospheric Chemistry Experiment (ACE), also known as SCISAT, is a Canadian-led mission supported mainly by the Canadian Space Agency and the Natural Sciences and Engineering Research Council of Canada; we thank Kaley Walker for helping us access the ACE data and advising us on its use. We are also indebted to

Anne K. Smith and William Randel for their comments and suggestions on the original version of this work; and to Marty Mlynczak and two anonymous reviewers for additional comments, all of which have resulted in an improved paper. The National Center for Atmospheric Research (NCAR) is sponsored by the U.S. National Science Foundation. R. R. Garcia and D. R. Marsh were supported in part by NASA grants X09AJ83G and NNX13AE33G, respectively. M. López-Puertas and B. Funke were supported by MINECO (Spain) under grant ESP2014-54362-P, and EC FEDER funds. WACCM is a component of NCAR's Community Earth System Model (CESM), which is supported by the National Science Foundation (NSF) and the Office of Science of the U.S. Department of Energy. Computing resources were provided by NCAR's Climate Simulation Laboratory, sponsored by NSF and other agencies. This research was enabled by the computational and storage resources of NCAR's Computational and Information Systems Laboratory (CISL). The model output and data used in this paper is listed in the references or available from the authors.

References

Ball, W. T., N. A. Krivova, Y. C. Unruh, J. D. Haigh and S. K. Solanki (2014), A new SATIRE-S Spectral Solar Irradiance reconstruction for solar cycles 21–23 and its implications for stratospheric ozone, *J. Atmos. Sci.,* **71**, 4086-4101, 2014.

Beagley, S. R., C. D. Boone, V. I. Fomichev, J. J. Jin, K. Semeniuk, J. C. McConnell, and P. F. Bernath (2010), First multi-year occultation observations of CO_2 in the MLT by ACE satellite: Observations and analysis using the extended CMAM, *Atmos. Chem. Phys*., **9**, 1133-1153.

Boone, C. D., R. Nassar, K. A. Walker, Y. Rochon (2005), Retrievals for the atmospheric chemistry experiment Fourier-transform spectrometer, *Appl. Opt*., **44** (33), 7218–7231.

Boone, C. D., Walker, K. A., and Bernath, P. F. (2013), Version 3 Retrievals for the Atmospheric Chemistry Experiment Fourier Transform Spectrometer (ACE-FTS). In *The Atmospheric Chemistry Experiment ACE at 10: A Solar Occultation Anthology*, A. Deepak Publishing, Hampton, Virginia, USA, 103–127.

Clerbaux, C. et al. (2008), CO measurements from the ACE-FTS satellite instrument: data analysis and validation using ground-based, airborne and spaceborne observations, *Atmos. Chem. Phys*., **8**, 2569–2594.

Emmert, J. T., M.H. Stephens, P. F. Bernath, D. P. Drob and C. D. Boone (2012), Observations of increasing carbon dioxide concentrations in the Earth's thermosphere, *Nature Geoscience,* **5**, 868–871, doi:10.1038/ngeo1626.

Ermolli, I., et al., Recent variability of the solar spectral irradiance and its impact on climate modeling, *Atmos. Chem. Phys*., **13**, 3945–3977, 2013.

448 Fischer, H., et al. (2008), MIPAS: An instrument for atmospheric and climate research,
449 *Atmos. Chem. Phys*., **8**, 2151–2188.

450 Funke, B. et al. (2009), Carbon monoxide distributions from the upper troposphere to the
451 mesosphere inferred from 4.7μm non-local thermal equilibrium emissions measured by
452 MIPAS on ENVISAT, *Atmos. Chem. Phys*., **9** (7), 2387–2411.

453 Garcia, R. R., D. R. Marsh, D. E. Kinnison, B. A. Boville, and F. Sassi (2007), Simulation
454 of secular trends in the middle atmosphere, 1950-2003, *J. Geophys. Res.,* **112**, D09301,
455 doi:10.1029/2006JD007485.

456 Garcia, R. R., M. López-Puertas, B. Funke, D. R. Marsh, D. E. Kinnison, A. K. Smith, and
457 F. González-Galindo (2014), On the distribution of CO_2 and CO in the mesosphere and
458 lower thermosphere, *J. Geophys. Res*., **119**, 5700-5718, doi:10.1002/2013JD021208.

459 Hoffmann, P., M. Rapp, W. Singer, and D. Keuer (2011), Trends of mesospheric gravity
460 waves at northern middle latitudes during summer, *J. Geophys. Res*., **116**, D00P08,
461 doi:10.1029/2011JD015717.

462 Krivova, N., S. K. Solanki, and Y. C. Unruh (2011), Towards a long-term record of solar
463 total and spectral irradiance. *J. Atmos. Sol.-Terr. Phys*., **73**, 223–234,
464 doi:10.1016/j.jastp.2009.11. 013.

465 Kunz, A., L. L. Pan, P. Konopka, D. E. Kinnison, and S. Tilmes (2011), Chemical and
466 dynamical discontinuity at the extratropical tropopause based on START08 and
467 WACCM analysis, J. *Geophys. Res*., **116**, D24302, doi:10.1029/2011JD016686.

Lean, J. L., G. J. Rottman, H. L. Kyle, T. N. Wood, J. R. Hickey and L. C. Puga (1997), Detection and parameterization of variations in solar mid- and near-ultraviolet radiation (200-400 nm), *J. Geophys. Res*., **102**, 29,329-29,956.

Liu, H.-L., F. Sassi and R. R. Garcia (2009), Error growth in a whole atmosphere climate model, *J. Atmos. Sci.,* **66**, 173-186.

Nedoluha, G. E., R. M. Gomez, B. C. Hicks, J. E. Wrotny, C. Boone, and Alyn Lambert (2009), Water vapor measurements in the mesosphere from Mauna Loa over solar cycle 23, *J. Geophys. Res.,* **114**, D23303, doi: 10.1029/2009JD012504.

Oelhaf, H., MIPAS Mission Plan (2008), ESA Technical Note ENVI- SPPA-EOPG-TN-07-0073.

Richter, J. H., F. Sassi, and R. R. Garcia (2010), Toward a physically based gravity wave source parameterization in a general circulation model, *J. Atmos. Sci.,* **67,** 136-156.

Rienecker, M. M., et al. (2011), MERRA: NASA's Modern-Era Retrospective Analysis for Research and Applications, *Journal of Climate*, **24**, 3624-3648, doi:10.1175/JCLI-D-11-00015.1.

Roble, R. G. (1995), Energetics of the mesosphere and thermosphere, in The Upper Mesosphere and Lower Thermosphere: A Review of Experiment and Theory, *Geophys. Monogr.* Ser., vol. **87**, edited by R. M. Johnson and T. L. Killeen, pp. 1–21, AGU, Washington, D. C., doi:10.1029/GM087p0001.

Smith, A. K., D. R. Marsh, M. G. Mlynczak, and J. C. Mast (2010): Temporal variations of atomic oxygen in the upper mesosphere from SABER, *J. Geophys. Res.*, **115**, D18309, doi:10.1029/2009JD013434.

490 Tiao, G. C., G. C. Reinsel, D. Xu, J. H. Pedrick, X. Zhu, A. J. Miller, J. J. DeLuisi, C. L.
491 Mateer, and D. J. Wuebbles (1990), Effects of autocorrelation and temporal sampling
492 schemes on estimates of trend and spatial correlation, *J. Geophys. Res.*, **95**, 20,507-
493 20,517.

494 Yue, J., J. Russell III, Y. Jian, L. Rezac, R. Garcia, M. López-Puertas, and M. G. Mlynczak
495 (2015), Increasing carbon dioxide concentration in the upper atmosphere observed by
496 SABER, *Geophys. Res. Lett*., **42**, doi:10.1002/2015GL064696.

497 Zhu, Y., M. Kaufmann, M. Ern, and M. Riese: Nighttime atomic oxygen in the mesopause
498 region retrieved from SCIAMACHY O(^{1}S) green line measurements and its response to
499 solar cycle variations (2015), *J. Geophys. Res.*, doi: 10.1002/2015JA021405.

500

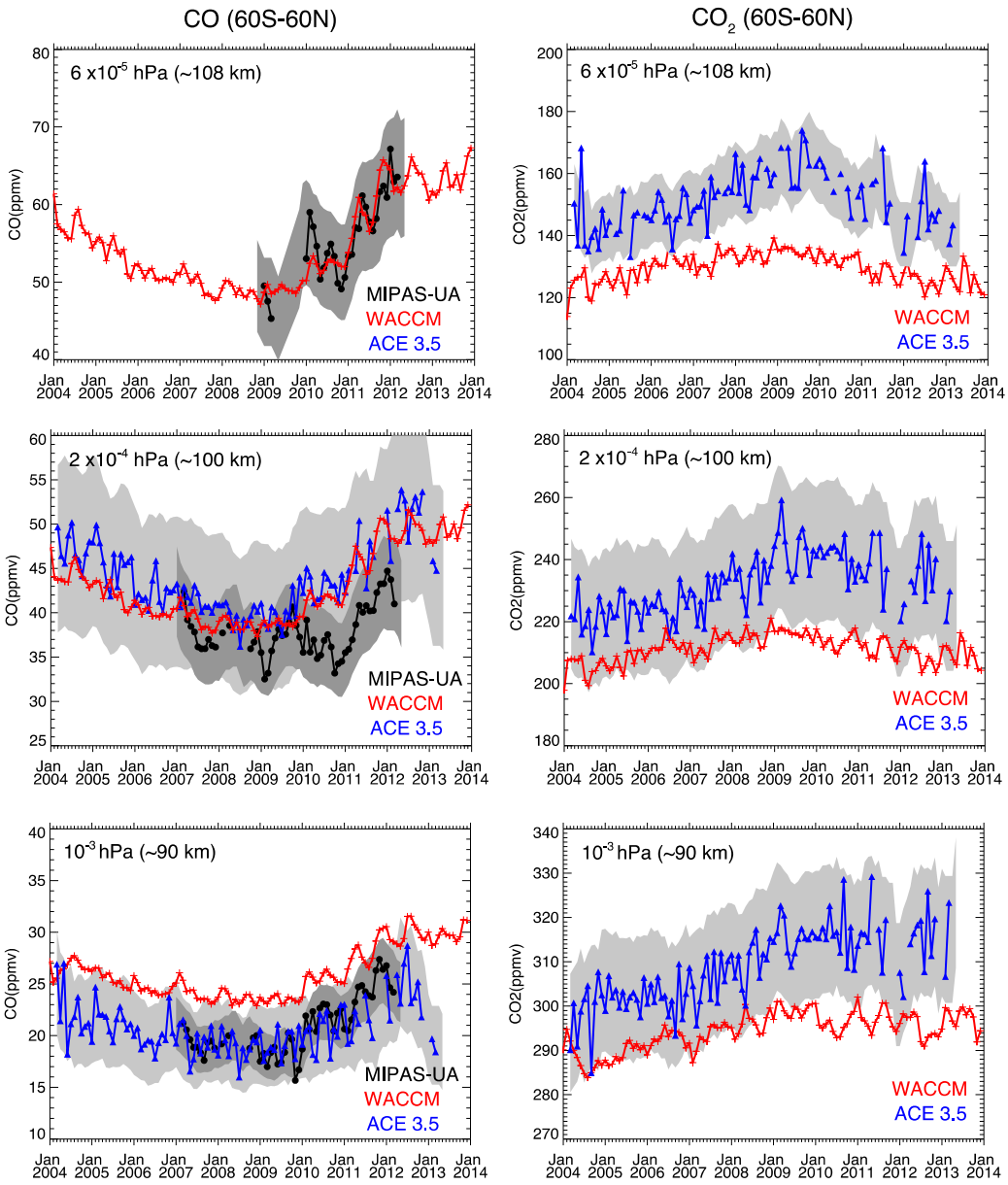

501

502 Figure 1. Evolution of observed and modeled CO (left) and CO_2 (right) averaged over 60S-
503 60N for 2004-2013 at three pressure levels. Black and blue curves denote MIPAS and ACE
504 data, respectively, with systematic measurement errors shaded; WACCM results are shown
505 in red.

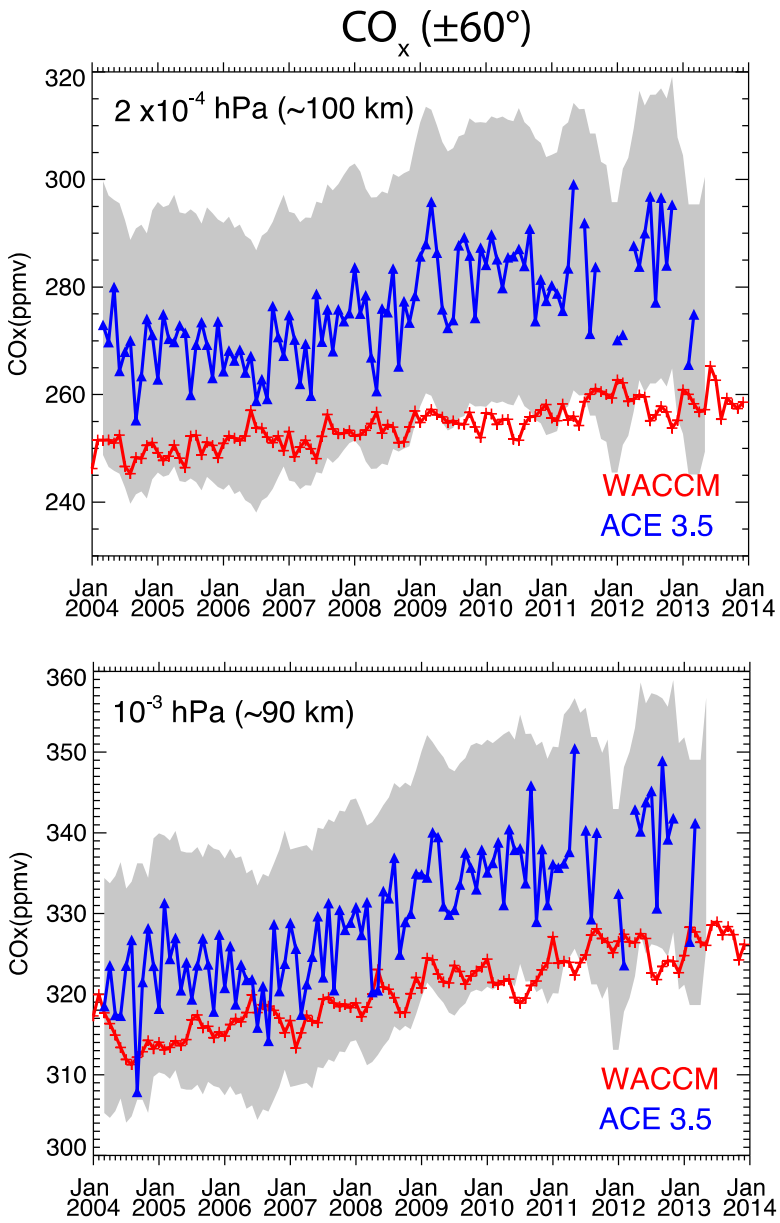

506

507 Figure 2. Evolution of observed and modeled CO_x averaged over 60S-60N for the period

508 2004-2013 at 2 x 10^{-4} hPa and 10^{-3} hPa. Blue curves denote ACE data, with systematic

509 errors shaded; WACCM results are shown in red.

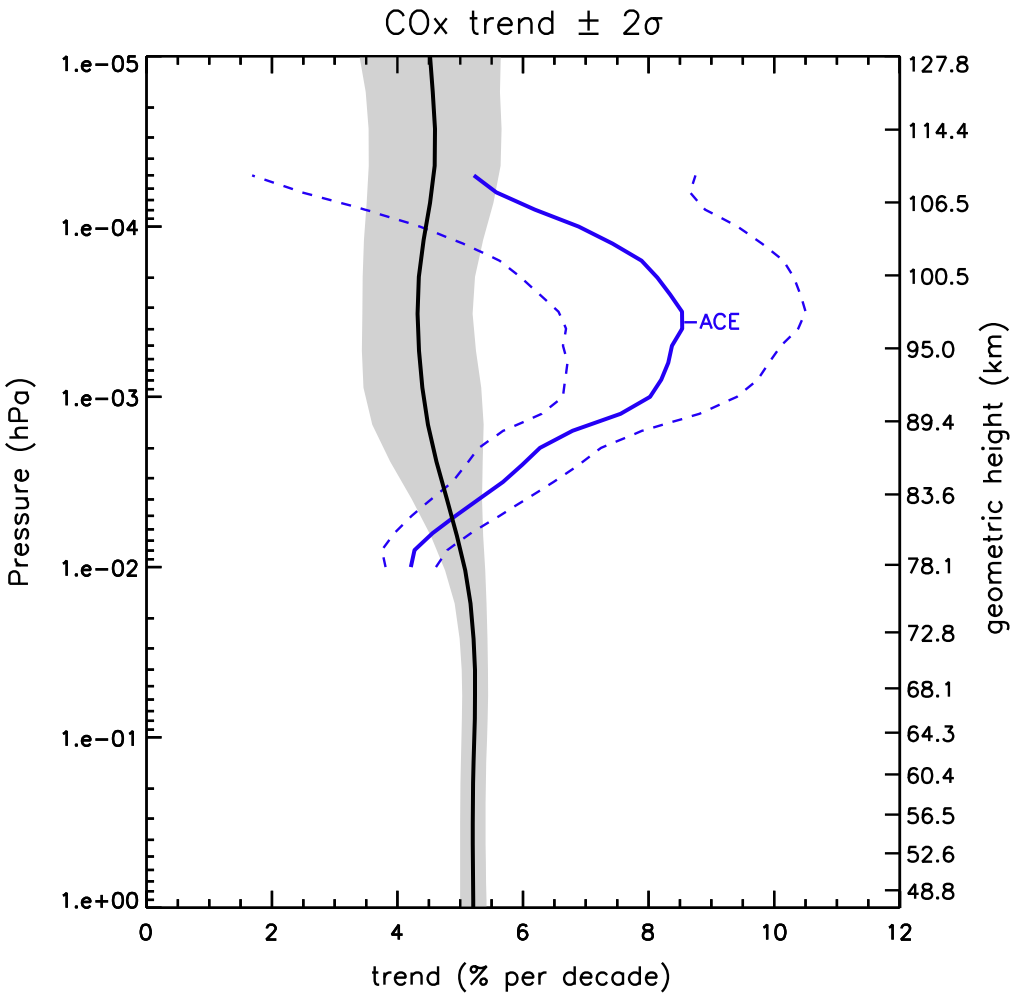

510

511 Figure 3. Vertical profile of the global trend (% per decade) of $CO_x = CO + CO_2$ for the

512 period 2004-2013 derived from ACE observations (blue) and WACCM results (black).

513 Dashed lines and gray shading denote 2-sigma uncertainties of the ACE and WACCM

514 trend estimates, respectively.

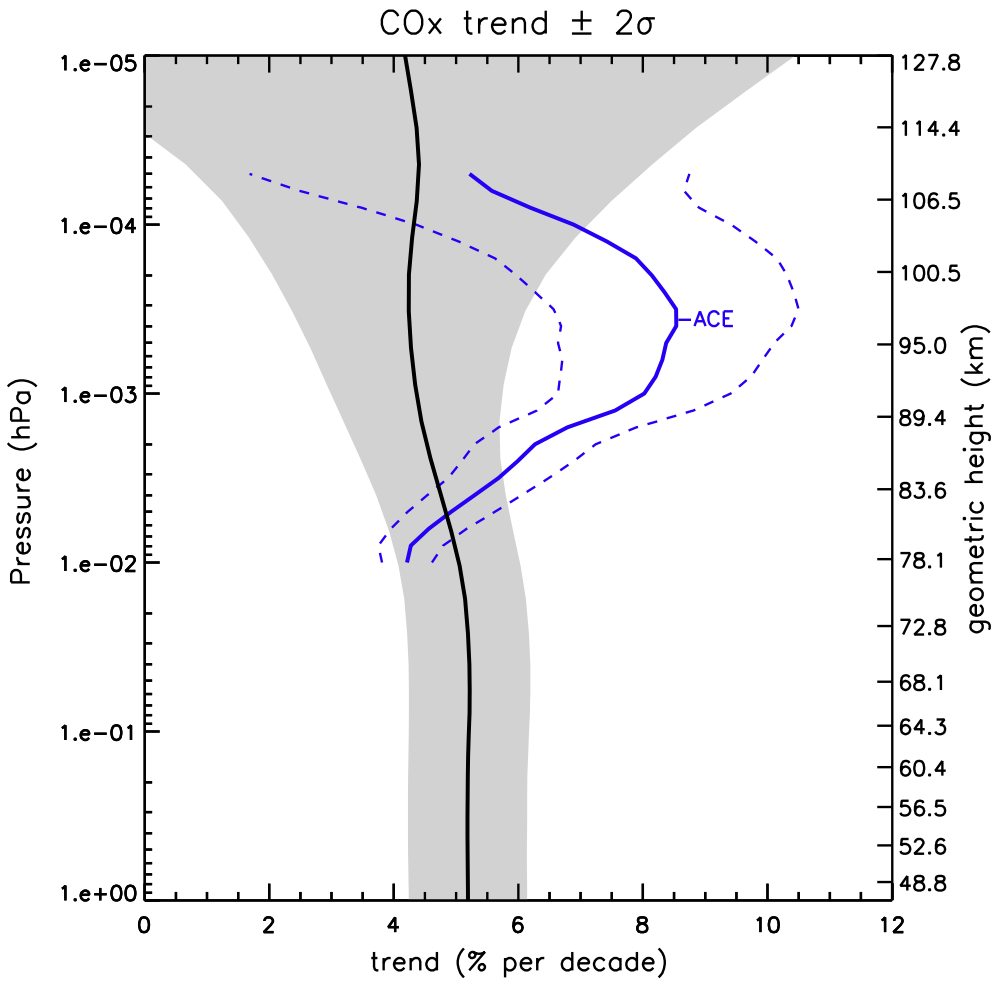

515

516 Figure 4. Effect on the WACCM CO_x trend of adding random noise to the model output.

517 The blue curve denotes the trend derived from ACE; dashed lines and gray shading denote

518 2-sigma uncertainties of the ACE and WACCM trend estimates, respectively. See text for

519 details.

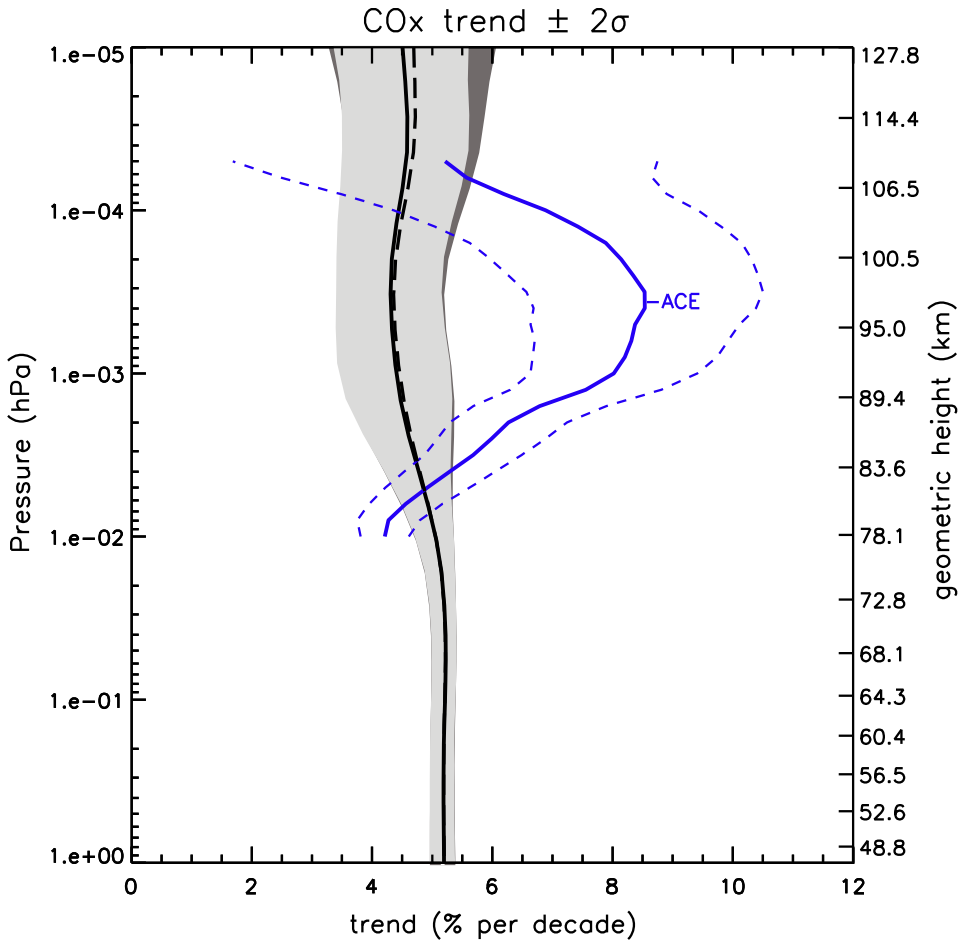

520

521 Figure 5. Effect on the WACCM CO_x trend of doubling the solar cycle irradiance variation
522 at 120-200 nm. The solid curve and light shading denote the trend from the original
523 simulation and its uncertainty; the dashed curved and dark shading refer to the simulation
524 with increased irradiance variability. The blue curve and dashed lines denote the ACE trend
525 and its uncertainty. See text for details.

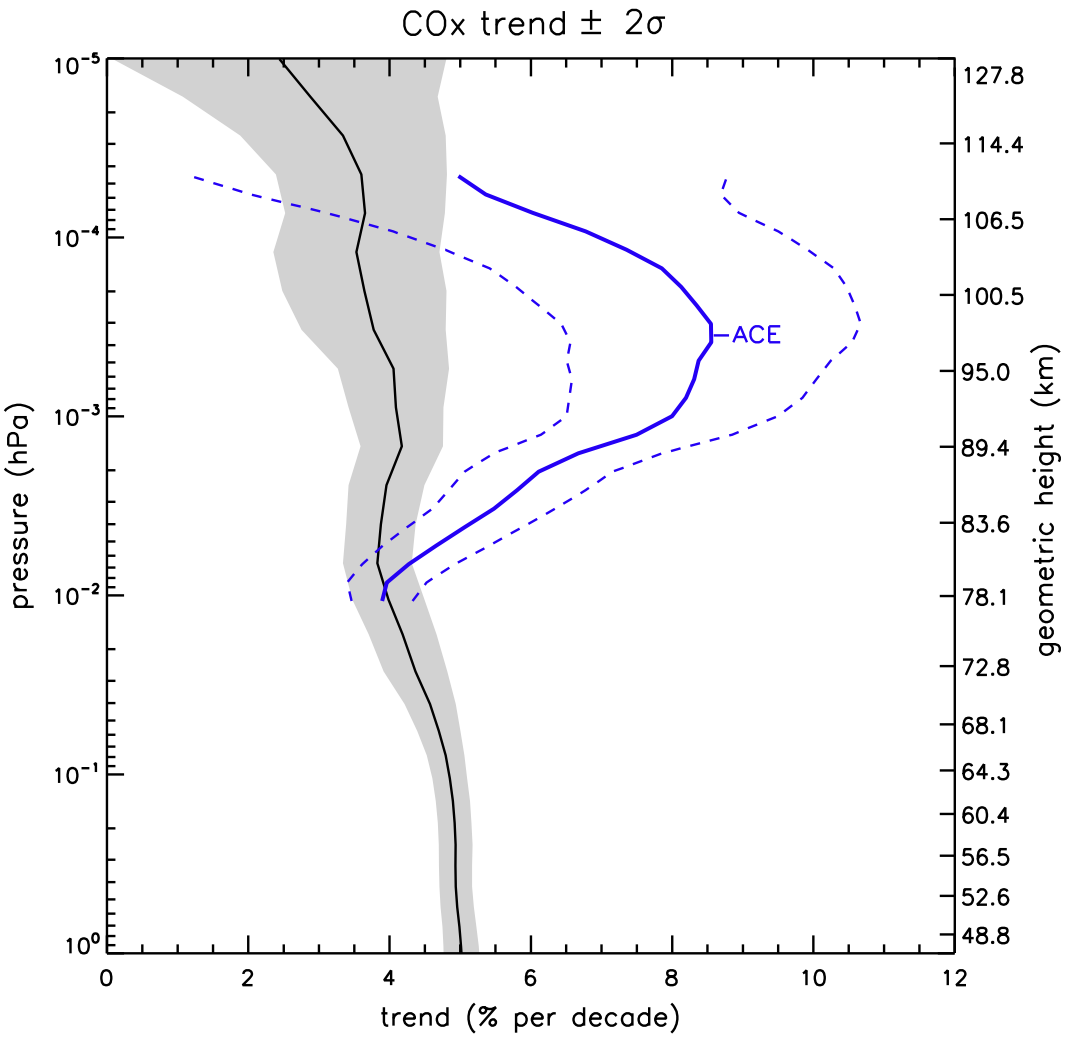

526

527 Figure 6. The WACCM CO_x trend obtained when the model is sampled at the geo-locations

528 of the ACE-FTS observations compared with the trend obtained from ACE data;

529 uncertainties are denoted by shading and dashed lines, respectively. See text for details.

530

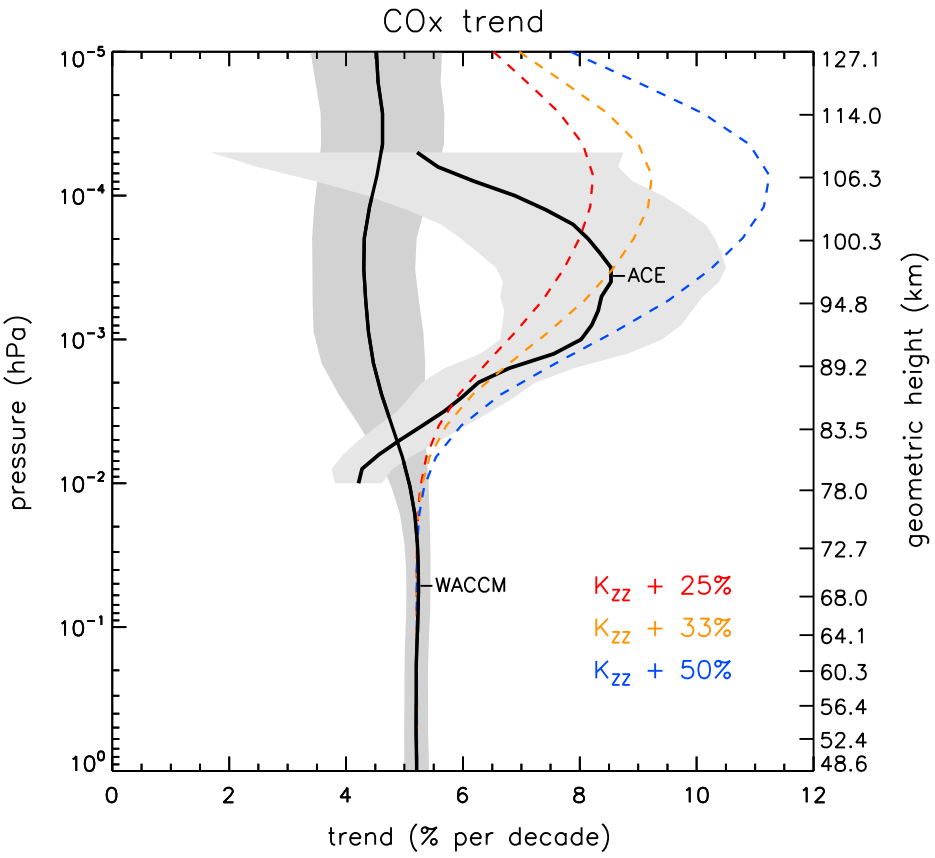

531

532 Figure 7. Effect of changing K_{zz} on the WACCM trend of CO_x. ACE and WACCM trends
533 for 2004-2013 are denoted by the black curves, with gray shading indicating 2-sigma
534 uncertainties. The estimated impact on WACCM results of increasing K_{zz} by 25%, 33% and
535 50% per decade is illustrated by the colored dashed curves. See text for details.

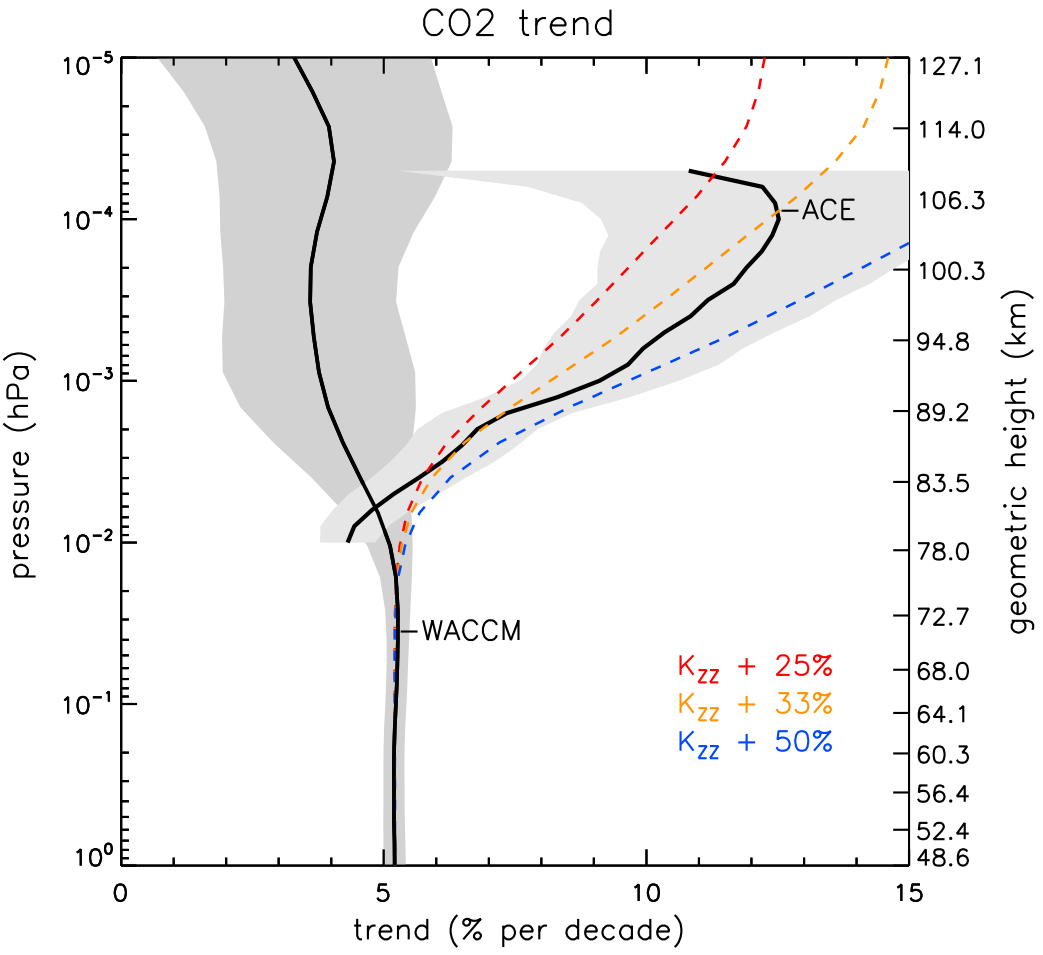

536

537 Figure 8. As in Figure 7, but for the trend of CO_2.

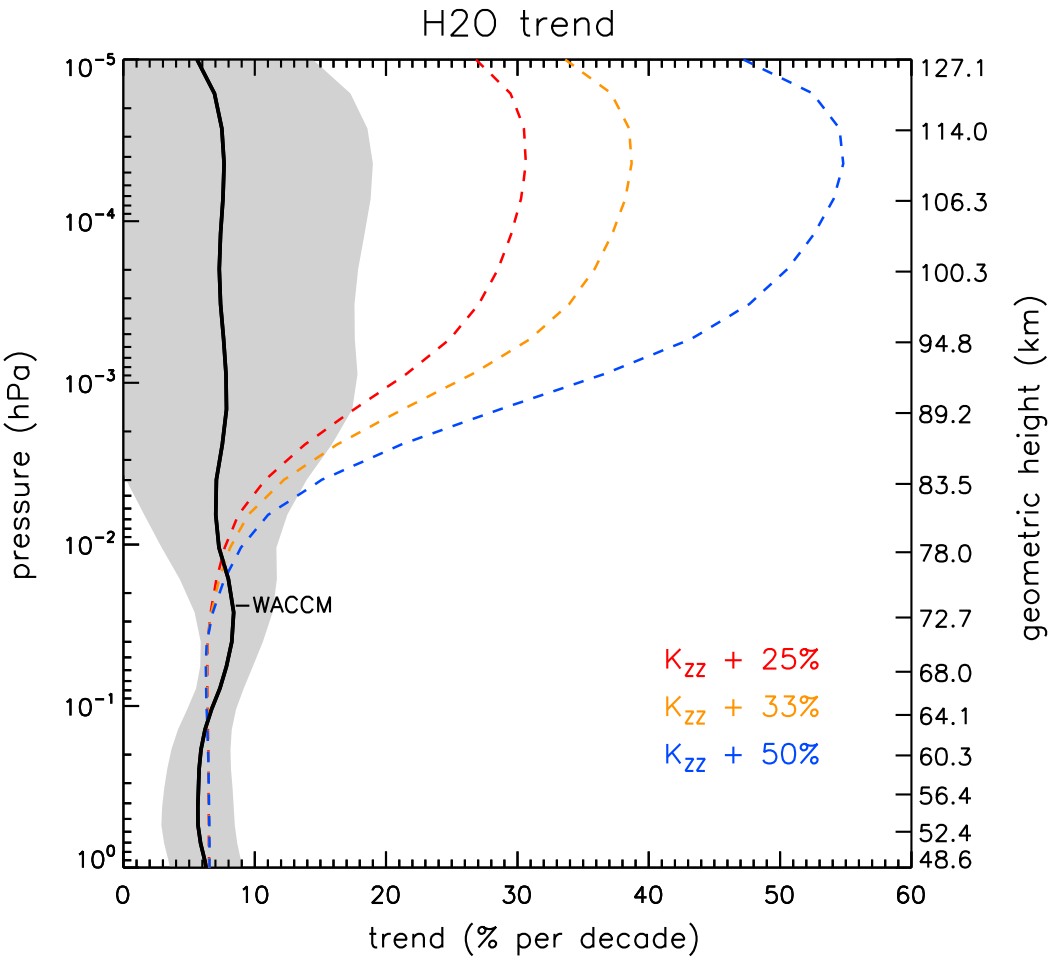

538

539 Figure 9. As in Figure 7, but for the trend of H_2O.